2003-01-0819

FTP and US06 Performance of Advanced High Cell Density Metallic Substrates as a Function of Varying Air/Fuel Modulation

Klaus Mueller-Haas, Rolf Brueck
EMITEC GmbH

Jeffery S. Rieck
Johnson Matthey

Cynthia C. Webb, Keith A. Shaw
Southwest Research Institute

ABSTRACT

The influence of catalyst volume, cell density and precious metal loading on the catalyst efficiency were investigated to design a low cost catalyst system. In a first experiment the specific loading was kept constant for a 500 cpsi and a 900 cpsi substrate. In a second experiment the palladium loading was reduced on the 900 cpsi substrate and the same PM loading was applied to a 1200 cpsi substrate with lower volume. Finally the loading was further reduced for the 1200 cpsi substrate. The following parameters were studied after aging:

– Catalyst performance of standard cell density compared to high cell density technology
– Light-off performance and catalyst efficiency as a function of Palladium loading and substrate cell density
– Catalyst efficiency as a function of AFR biasing

The performance of the aged catalysts was investigated in a lambda sweep test and in light-off tests at an engine bench. After pre-testing the catalyst were installed in a MY 2002 – V 6 vehicle to compare the performance of the aged catalysts during the FTP and US06 test cycle before and after AFR adjustments.

The test results show advantages of high cell density substrates during FTP cold start and during hot transient condition. The volume of high cell density catalyst can be reduced as compared to standard cell density substrates due to the higher specific efficiency. The palladium loading of high cell density technology can be reduced as a result of faster heat up and faster light-off during FTP cold start compared to 500 cpsi catalysts. The results also demonstrate the sensitivity of emission reduction to air-fuel ratio for high cell density converters.

INTRODUCTION

The relationship between the geometric surface area, volume and cell density was published earlier in [1, 2, 3]. Future legislations, especially PZEV applications, require fast catalyst light off and higher catalyst efficiency after the warmed up phase. Catalyst light-off can be improved with higher cell density substrates and reduced wall thickness. Increasing catalyst volume or/and cell density and precious metal loading will improve the overall catalyst efficiency. The advantage of higher cell density substrates with higher specific geometric surface area and lower heat capacity is seen through higher efficiencies per volume compared to standard cell densities due to the better mass transfer by smaller hydraulic diameter.

The objective of this work was to layout a low cost catalyst system with the same catalyst efficiency by optimization of catalyst volume, precious metals and cell density at the same flow resistance. Several substrates were applied with different loadings and similar washcoat. Lambda sweep tests with varied A/F frequency and amplitude were conducted in order to identify the best calibration for the catalyst. All substrates were aged and tested over the FTP as well as the US06 test cycle on a production vehicle equipped with a V6 3.5 ltr engine. The catalysts were retested in the FTP cycle with AFR biased calibration. The AFR perturbation, meaning lambda frequency and amplitude, were not changed. Also, The fuel consumption of the vehicle in the FTP and the US06 were unchanged.

Tested Substrates and PGM loading

Table 1 summarizes the physical properties of the substrates. The transversal foil structure (TS) was used for the 500 cpsi substrate to improve the heat transfer during the heat up phase and increase the mass transfer during the warmed up phase [5]. In addition, 900 cpsi and 1200 cpsi substrates were tested. The catalyst length was reduced to keep the back pressure similar. The foil thickness was reduced for the 1200 cpsi substrate to keep the thermal mass similar compared to the 900 cpsi substrate. No further light-off improvements would be expected without reduction of the foil thickness of the 1200 cpsi substrate [4].

ID		M500	M900	M1200
Cell Density	[cpsi]	500 TS	900	1200
Wall Thickness	[µm]	30	30	25
Diameter	[mm]	98.4	98.4	98.4
Length	[mm]	130	113	101.5
Volume	[ltr]	1.0	0.86	0.77
GSA	[sqm]	3.6	3.7	3.8
OFA	[%]	75	74	75
Thermal Mass (1”)	[J/K]	93	108	107
PGM Loading		HL	HL/ LL	LL/ LLL

Table 1: Physical properties of the tested substrates

Figure 1 shows the relative amount of precious metals, which were applied to the different substrates. The specific loading “high load” (HL) was kept constant for the 500 cpsi and the 900 cpsi substrate. A second loading level "low load” (LL) was used for the 900 cpsi and 1200 cpsi substrate where the palladium level was reduced by 47 %. The 1200 LLL catalyst had additional reduced Palladium level but slightly higher Platinum level. The same washcoat technologies were used for all substrates.

The coated substrates were canned with identical cones and insulated with an air-gapped heat shield. Thermo-couples were installed to record catalyst exhaust gas inlet temperature and bed temperature during aging and during emission testing. Emission sample probe lines were used to analyze feed gas and tail pipe emissions.

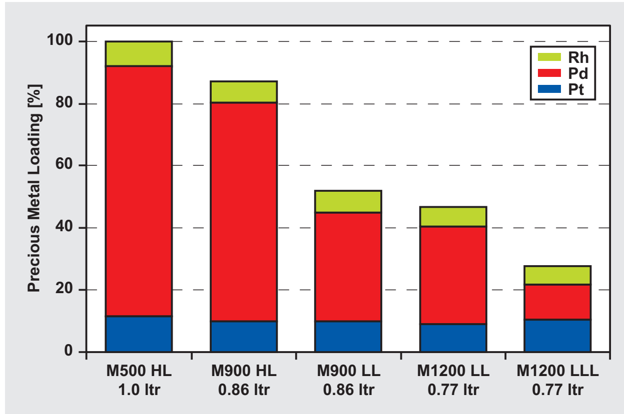

Figure 1: Relative amount of precious metals for the tested substrates

Catalyst Aging Procedure

Four catalysts were aged in parallel on an engine bench equipped with 7.5 ltr V8 engine in a two mode aging cycle. All converters were aged to a 50 k road aging condition. During mode one, catalyst bed temperature was below 700 °C at rich exhaust gas condition. The catalyst bed temperatures increase above 1000 °C during mode two at lean exhaust condition. Exhaust gas mass flow was constant for all converters during the aging cycle. The bed temperatures, air-fuel ratio and engine variables were controlled and recorded at 1 Hz during cycling.

Emission Testing

The emission performance of each converter was studied in two steps. In the first step the lambda sweep test and light-off test was conducted to determine the character of the aged substrates. After engine bench testing the catalyst efficiency were measured in the vehicle during the FTP75 and US06 test cycle.

Lambda Sweep and Light-Off Test

The purpose of the Flexible Exhaust Evaluation Rig (FLEXER) tests was to evaluate the stabilized con-version efficiency of each catalyst as a function of AFR. During a FLEXER test, both exhaust flow rate and inlet gas temperature to the test catalyst are closed-loop controlled by a PC-based data acquisition system. For the tests, the exhaust flow rate is held constant and the exhaust gas temperature and/or AFR at the inlet to the test catalyst is controlled to a user defined ramp. During the test, before and after catalyst exhaust gas concentrations of THC, CO, NO_X and O_2 are measured at 1 Hz. The dynamic AFR sweep test is achieved by slowly ramping the engine fuel from a rich condition (AFR<13.6) to a lean condition (AFR>14.6) while monitoring catalyst conversion efficiency for of HC, CO and NO_X.

Figure 2 shows the measured conversion efficiency of the aged 900 HL catalyst during the dynamic AFR-sweep test, with the inlet exhaust gas temperature adjusted to 650 °C. It can be seen that the slope of the NO_X efficiency on the lean side is very sharp. The CO conversion rate also decreases very rapidly on the rich side. For this catalyst, maximum catalyst efficiency for all three pollutants is achieved at a mean AFR between 14.52 and 14.54.

The 900 HL and the 900 LL converter where tested at a AFR perturbation of 1 Hz and ±1 AFR.

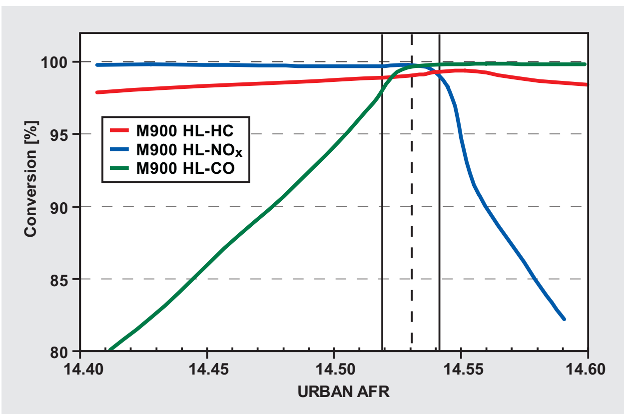

Figure 2: Air/Fuel Sweep – 900 cpsi HL catalyst (exhaust gas temperature 650 °C, mass flow 49 scfm, AFR perturbation 1Hz, ±1 AFR)

Figure 3 shows the catalyst efficiency during the Air/Fuel Sweep test for both converters. The CO and NO_X conversion is minor influenced but the HC efficiency decreased for the lower loaded catalyst (900 LL). A second test on the run on the rig is used to assess the light-off temperature of each converter. The HC-light-off temperature was about 22 Kelvin higher for the 900 LL converter.

Baseline Vehicle Performance

The test vehicle used in this test program was a 2002 DaimlerChrysler 300 M with a 3.5 ltr engine. The vehicle was aged to 4,500 miles prior to testing. The test vehicle installed in the test facility is shown in Figure 5.

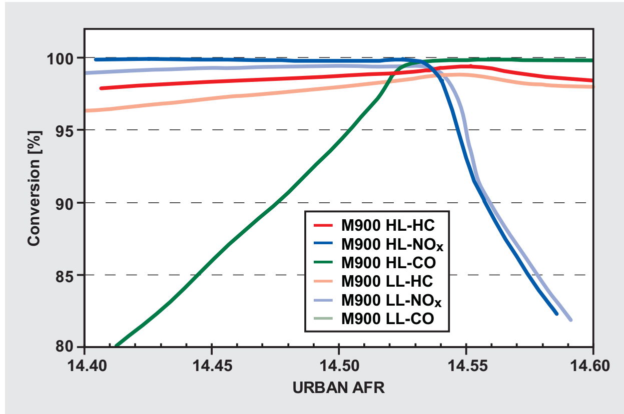

Figure 3: Air/Fuel Sweep – Example – 900 HL aged compared to 900 LL aged (exhaust gas temperature 650 °C, mass flow 49 scfm, AFR perturbation 1 Hz, ±1 AFR)

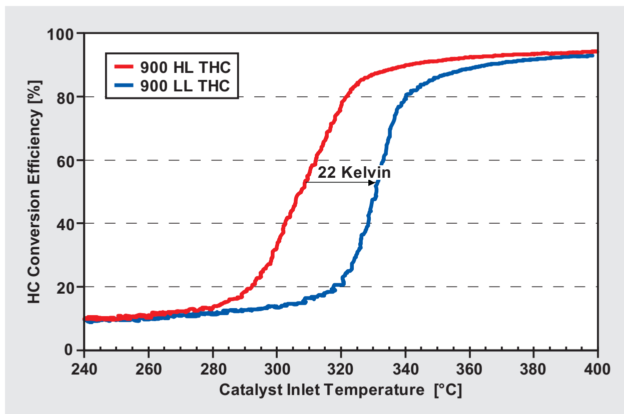

Figure 4: HC- light-off of the 900 HL and 900 LL catalyst after aging (mass flow=20 scfm, AFR=14.67, temperature transient=20 K/min)

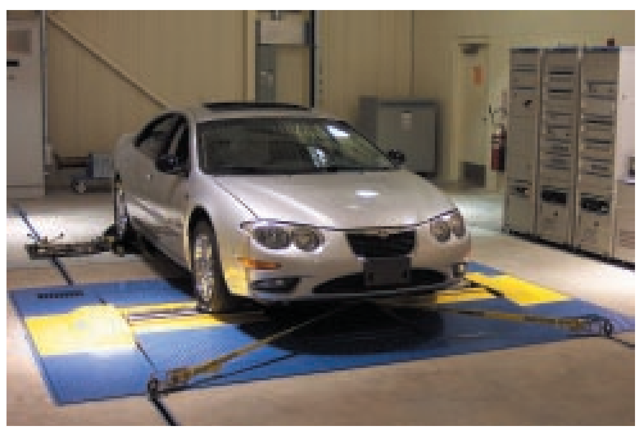

Figure 5: Program Test Vehicle

The catalysts were installed in close coupled position. After the vehicle was prepared for the test work, the FTP and US06 emissions were measured. The measured exhaust gas inlet temperature and the engine mass flow are shown in Figure 6.

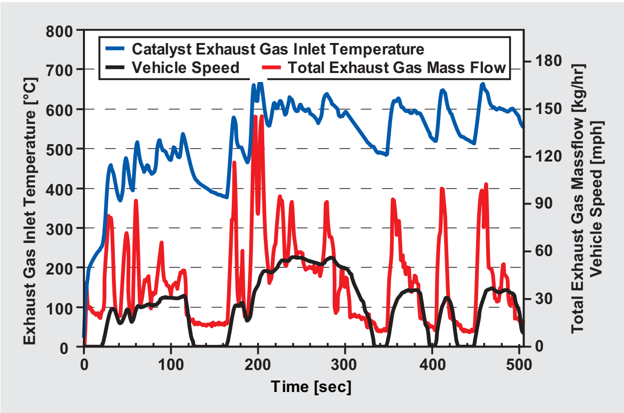

Figure 6: Exhaust gas temperature and exhaust gas mass flow during FTP cold start

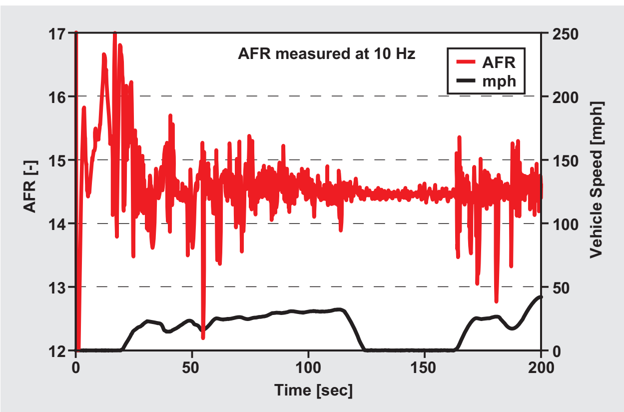

Figure 7: Engine AFR during FTP cold start

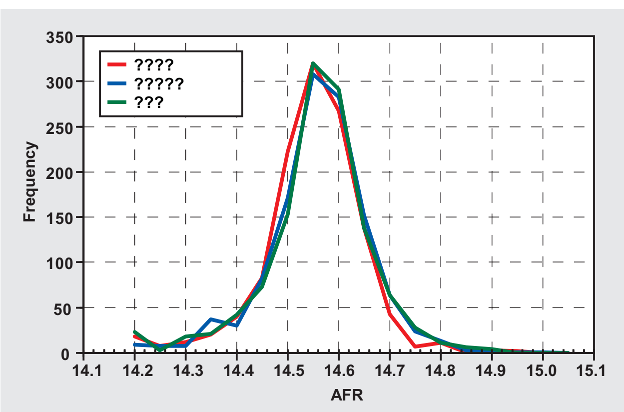

Figure 8: AFR distribution during the time period 100 to 1374 seconds during FTP testing

The figure shows that the inlet temperature to the catalyst is between 400 to 500 ºC for the first 150 seconds, after which it typically ranges between 500 to 650 °C. The vehicle operates open-loop during the first 30 seconds of the cold-start portion of the FTP cycle. The measured AFR during FTP cold start is shown in Figure 7.

Before integrating the catalyst systems with the engine AFR controls, the base AFR control was characterized. The catalyst efficiency during hot transient condition is highly influenced by the engine AFR control. Therefore, a vehicle with consistent AFR control is necessary to make good emission reduction comparisons for different catalyst systems. Figure 8 shows the distribution of the AFR for three FTP tests for the time period 100 to 1374 seconds. The mean AFR is about 14.54 for all test and verifies the repeatability of the tests with the OEM calibration.

Influence of Engine Calibration

After each catalyst was AFR sweep tested on the FLEXER rig, the FTP and US06 emissions were tested on the vehicle using the stock engine calibration. The optimum AFR set point was determined by comparing the average AFR measured on the vehicle with the sweep test results obtained using FLEXER. Both the vehicle and the bench engine were operated on the same batch of EEE-clear gasoline. This allowed for a direct comparison between the two test stands. Figure 9 shows the position of the average AFR measured on the vehicle compared to the sweep data. This figure shows that the NO_X performance should improve with the average exhaust AFR shifted slightly richer than the average AFR measured on the vehicle. To test this hypothesis, the AFR control on the vehicle was manipulated to shift the average AFR rich by 0.03 AFR [6]. The result of this AFR bias shift lowered overall average NO_X mass emissions substantially, moving the Phase 2 (bag 2 of the FTP test cycle) NO_X conversion efficiency from 98 percent increased to 99 percent.

The FTP emission test results as a function of AFR set point are shown in Figure 10. The NO_X mass emissions were more sensitive to the bias shift than the NMHC and CO tailpipe emissions. In the stock configuration (with the average AFR equal to 14.54) the Bag 2 catalyst efficiencies were 99.6, 99.5, and 98.1 percent for THC, CO and NO_X respectively. For the bias shifted to an average AFR of 14.51, the Bag 2 efficiencies were 99.7, 98.5, and 99.1 for THC, CO and NO_X of the FTP bag 2 conversion efficiencies, respectively. Reexamining the sweep (Figure 9) it was determined at a shift of –0.02 AFR would probably maximize the three-way efficiency. At an average AFR of 14.52 all three were above 99 percent. The FTP results correlate well

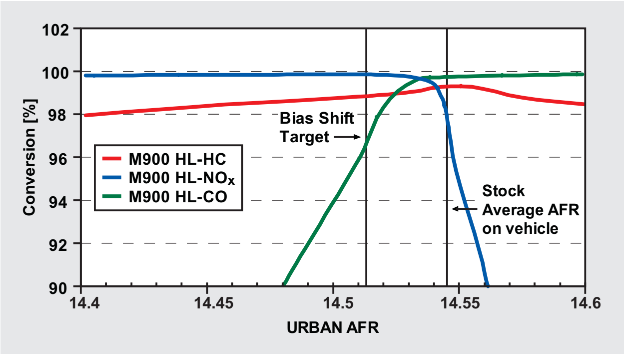

Figure 9: AFR Sweep data shown with average stock and average target AFR

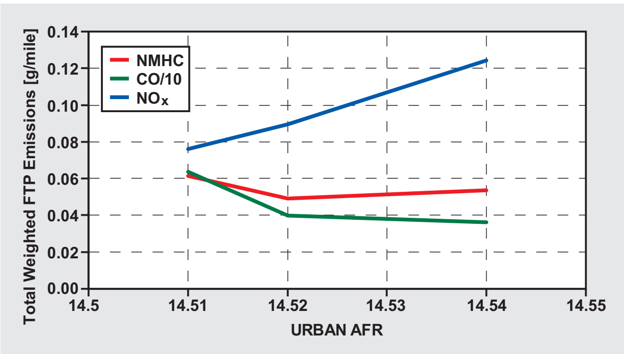

Figure 10: Total FTP Emissions results depending on AFR bias

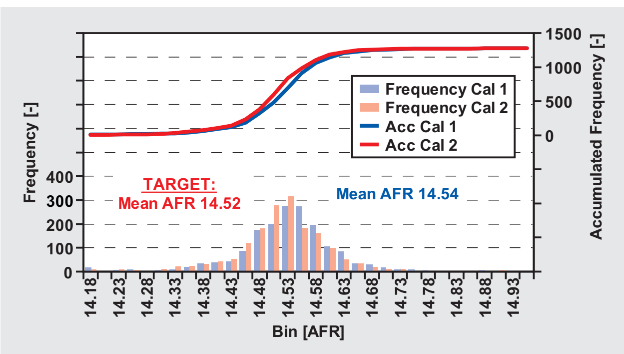

Figure 11: AFR distribution and cumulative distribution of calibration 1 and calibration 2 (FTP test)

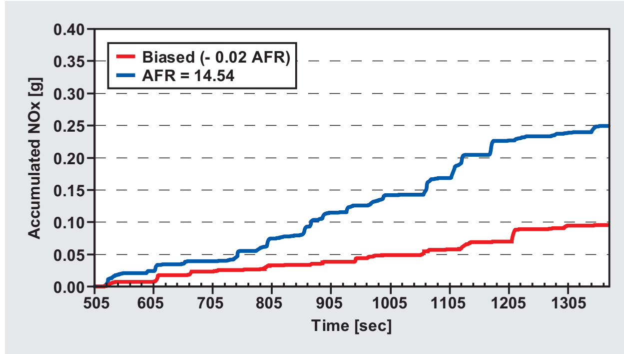

Figure 12: Accumulated NO_X-emissions during the second phase of the FTP with stock calibration and biased AFR (900 HL catalyst)

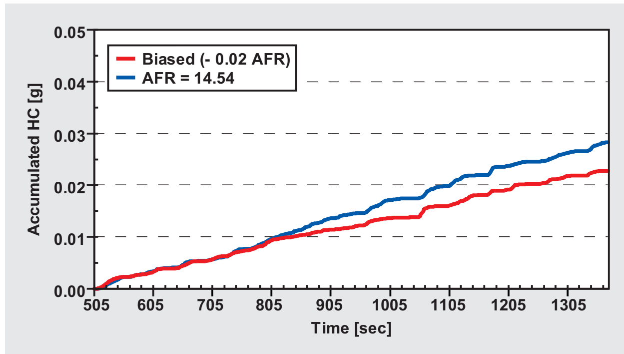

Figure 13: Accumulated HC- emissions during the second phase of the FTP with stock calibration and biased AFR (900 HL catalyst)

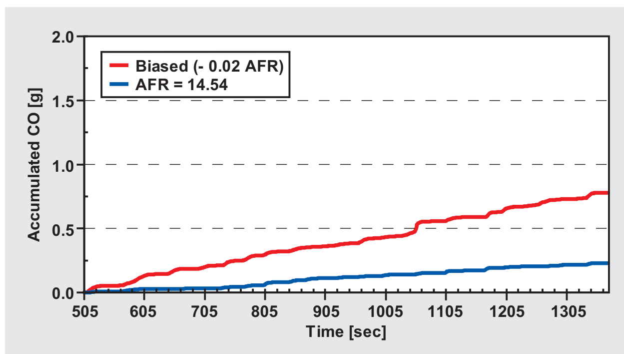

Figure 14: Accumulated CO- emissions during the second phase of the FTP with stock calibration and biased AFR (900 HL catalyst)

with the test results obtained on the FLEXER (compare with Figure 9). Figure 11 illustrates the Lambda distribution over phase 2 of the FTP before and after AFR biasing.

The accumulated tail pipe FTP emissions during the second phase of the FTP test cycle are shown in Figure 12 to 14. The figures show the effect of biasing on the instantaneous NO_X, HC and CO mass accumulation. It can be seen that NO_X mass control was greatly influenced by the slightly richer AFR. The CO emissions were increased after biasing.

All the remaining catalysts in the program were tested with the –0.02 AFR adjustment. The evaluations of groups of catalysts are described in the following sections.

Catalyst Development

The catalyst development strategy is schematically shown in Figure 15. The substrate cell density was increased from 500 cpsi to 900 cpsi and 1200 cpsi and the precious metal loading successive reduced. The development are divided in four stages:

Stage 1: The specific loading was kept constant for a 900 cpsi and the 500 cpsi substrate (HL). The reduction of precious metal is based on the 14 % lower volume of the 900 cpsi converter.

Stage 2: Same substrate design for both systems. Reduced Palladium loading for the 900 LL converter.

Stage 3: The specific loading was kept constant for a 1200 cpsi and the 900 cpsi substrate (LL). The amount of the precious metal is 10 % lower for the 1200 cpsi design through reduced volume.

Stage 4: Same substrate design for both systems. Slightly increased Platinum, same Rhodium level and reduced Palladium level for the 1200 LLL converter.

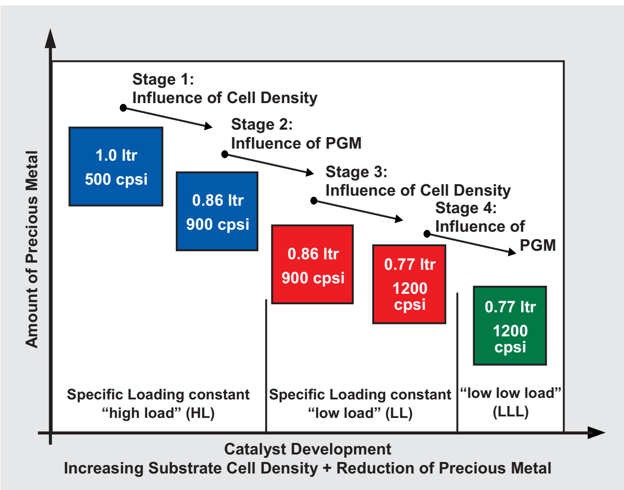

Figure 15: Catalyst development strategy

Stage 1: 900 HL compared to 500 HL

The THC-light-off of the 500 cpsi and the 900 cpsi catalyst is compared in Figure 16. The 900 cpsi catalyst shows an advantage during the first 100 seconds. A higher HC efficiency was realized between 40 and 100 seconds, which is attributed to the larger active GSA of the 900 cpsi catalyst. The accumulated HC, CO and NO_X emissions during the 1st FTP phase are shown in Figure 16, 17 and 18. The accumulated THC after the 900 cpsi catalyst is 20 % lower compared to the 500 cpsi catalyst. The advantage of the higher cell density 900 cpsi catalyst was also observed in the accumulated CO and NO_X tail pipe emissions.

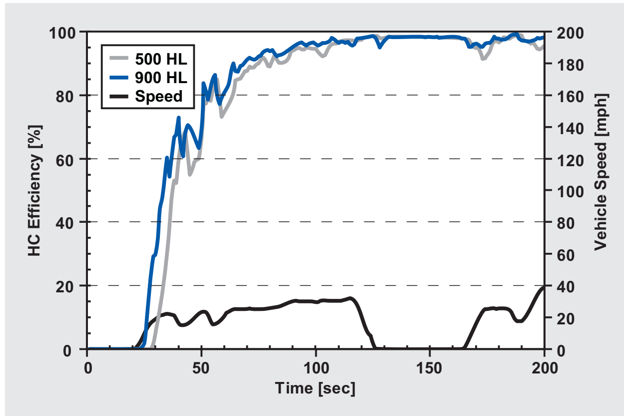

Figure 16: HC light-off during FTP cold start

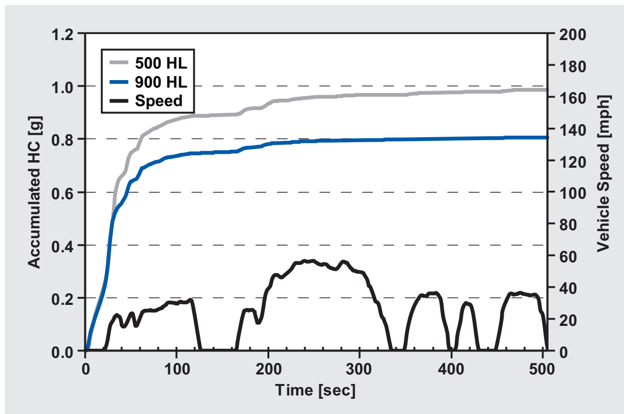

Figure 17: Accumulated HC during 1st Phase of the FTP test cycle (high load)

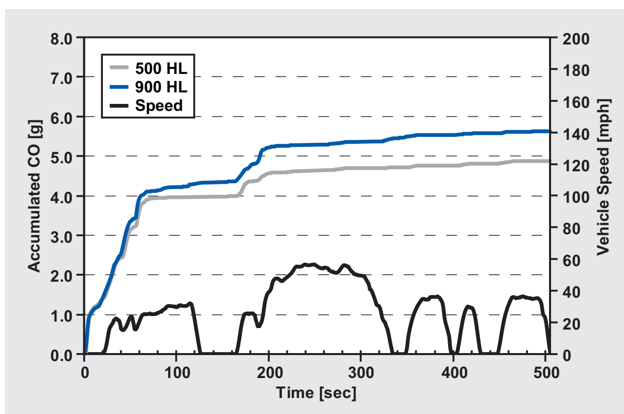

Figure 18: Accumulated CO during 1st Phase of the FTP test cycle (high load)

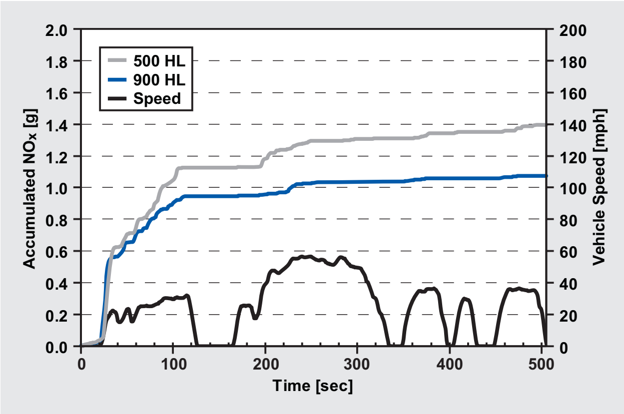

Figure 19: Accumulated NO_X during 1st Phase of the FTP test cycle (high load)

The temperature distribution after 60 second of the FTP cold start was calculated for both substrates and is shown in Figure 20. The temperature above 350 ºC is designated as a solid area at this time. The 900 cpsi substrate shows a 19 % higher GSA-activity compared to the 500 cpsi substrate.

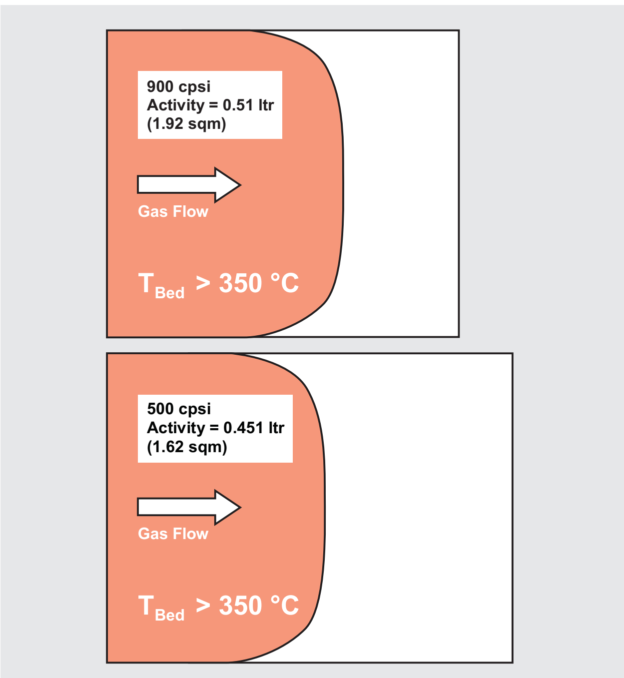

Figure 20: Calculated active Volume and geometric surface area of the 500 cpsi and 900 cpsi substrate 60 seconds after FTP cold start

The bag data are compared in Figure 21. The overall emission performance of the 900 cpsi catalyst was better. The HC and NO_X emissions during Bag one are lower and the CO emissions are slightly higher for the

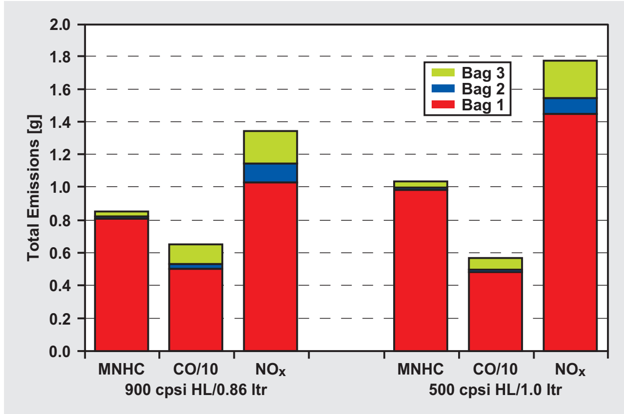

Figure 21: Emission bag data 500 cpsi catalyst compared to 900 cpsi catalyst

900 cpsi catalyst compared to the 500 cpsi system. The emissions results during the 2nd and 3rd phase of the FTP 75 test are similar for both designs.

Stage 2: 900 LL compared to 900 HL

Two Palladium levels were tested on the 900 cpsi substrate. The 900 LL catalyst was coated with about 50 % lower Palladium compared to the 900 HL catalyst. The substrate design and the canning of the system were identical.

The HC light-off performance of the two catalysts is compared in Figure 22. The 900 HL converter lights off faster than the 900 LL converter during the FTP cold start. This advantage is directly attributable to the lower catalyst light-off temperature through the higher Pd content (compare Figure 4). The earlier light-off result in lower THC accumulation during the first 100 seconds which is shown in Figure 23. The tail pipe NO_X emissions, shown in Figure 25, are not much influenced by the lower Palladium level.

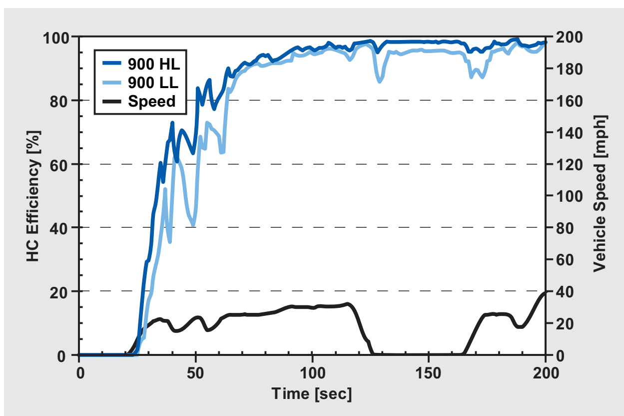

Figure 22: HC-Efficiency during FTP Cold Start depending on Palladium loading

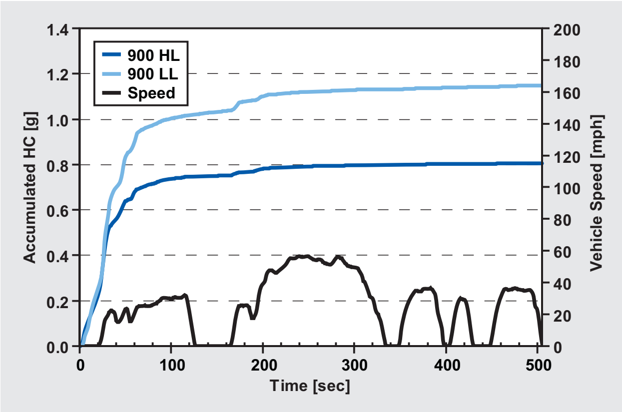

Figure 23: Accumulated HC after the 900 cpsi catalyst during 1st Phase of the FTP test cycle depending on Pd loading

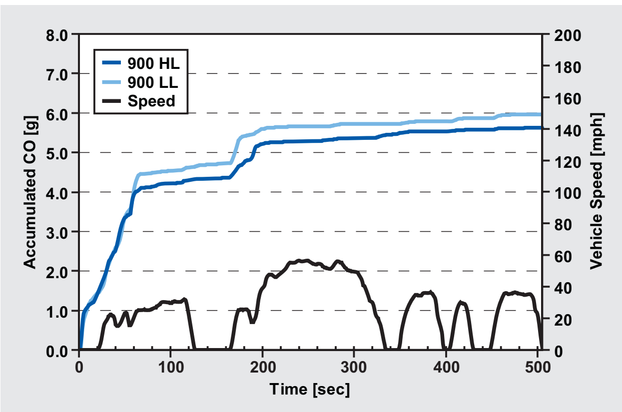

Figure 24: Accumulated CO after the 900 cpsi catalyst during 1st Phase of the FTP test cycle depending on Pd loading

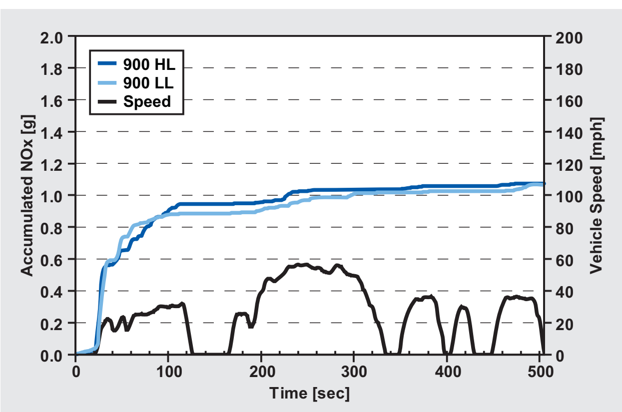

Figure 25: Accumulated NOx after the 900 cpsi catalyst during 1st Phase of the FTP test cycle depending on Pd loading

The total bag data are summarized in Figure 26. The Bag 1 NMHC data for the 900 LL catalyst are 40 % higher compared to the 900 HL catalyst. The CO and NO_X emissions are only slightly influenced. No major HC- and CO differences were achieved in bag two and three.

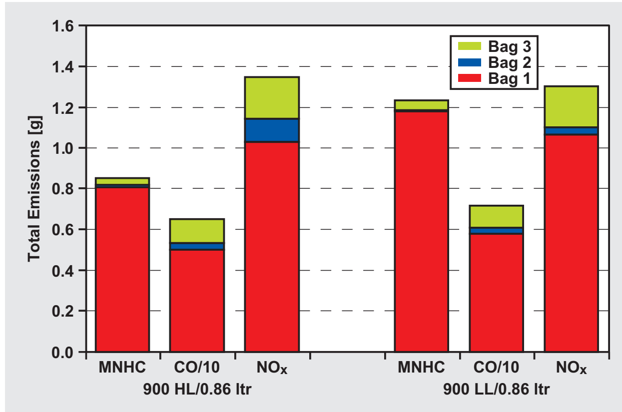

Figure 26: FTP-Emission bag data depending on Pd loading

Stage 3: 1200 LL compared to 900 LL

The 1200 LL catalyst was tested after the 900 cpsi catalyst. The volume of the 1200 LL converter was about 10 % lower than the 900 LL converter and the specific loading of precious metals equal for both. Therefore, there was a reduction of noble metals on the 1200 due to the volume reduction.

The light-off performance of both catalysts is compared in Figure 27. The 1200 cpsi catalyst shows a light-off advantage over the 900 cpsi catalyst. The faster light-off results in higher catalyst conversion rate (for HC, CO and NO_X) during the first 70 seconds.

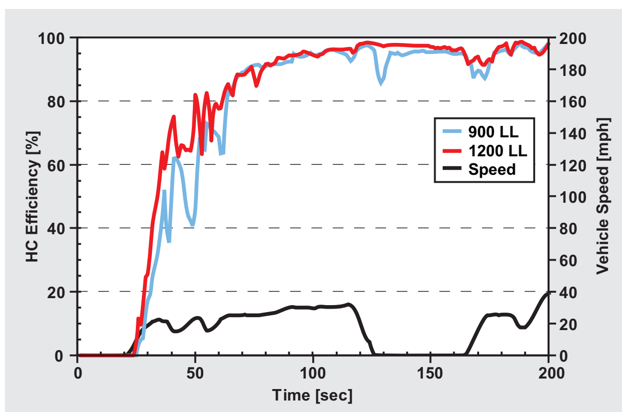

Figure 27: HC light-off performance of the 900 cpsi and 1200 cpsi catalyst during FTP cold start

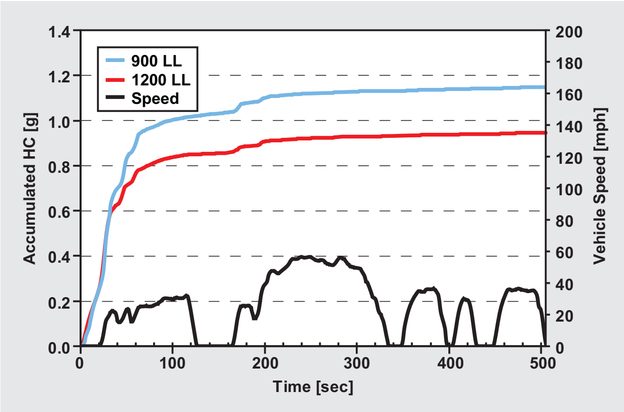

Figure 28: Accumulated HC after the 900 cpsi and 1200 cpsi catalyst during 1st Phase of the FTP test cycle (low load)

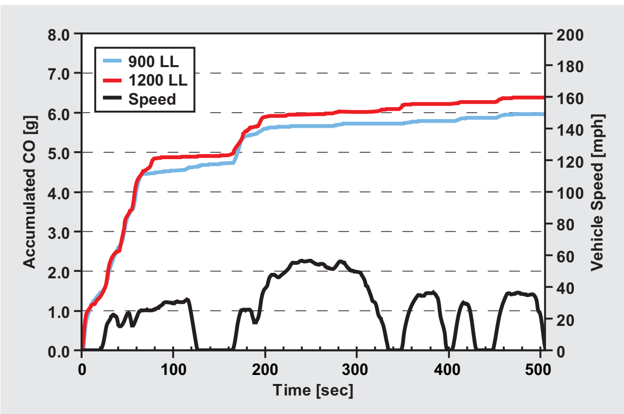

Figure 29: Accumulated CO after the 900 cpsi and 1200 cpsi catalyst during 1st Phase of the FTP test cycle (low load)

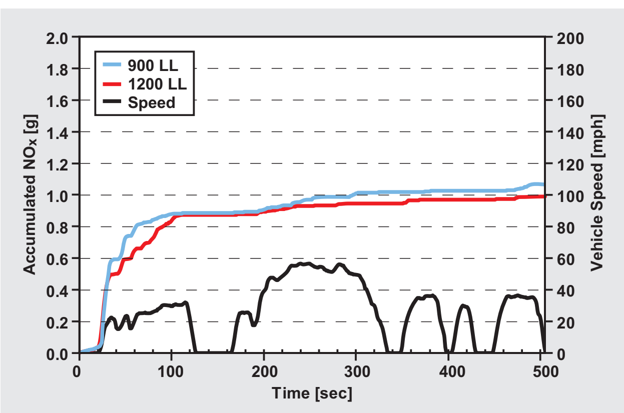

Figure 30: Accumulated NO_X after the 900 cpsi and 1200 cpsi catalyst during 1st Phase of the FTP test cycle (low load)

Figure 28 through 29 show the accumulated mass of THC, CO and NO_X during the first phase of FTP cycle. The accumulated hydrocarbon after the 1200 cpsi catalyst is about 20 % lower compared to the 900 cpsi catalyst. There is no major difference in the accumulated NO_X and CO emissions.

Figure 31 shows the emission data by bag for each FTP phase. The NMHC of the 1200 cpsi catalyst in bag 1 is lower compared to the 900 cpsi catalyst. NO_X emissions are slightly higher of the 1200 cpsi catalyst in phase two and three. The difference in performance between the 900 LL and the 1200 LL is attributed to the smaller hydraulic diameter and a better mass transfer in the warmed up condition and the better heat transfer in the FTP cold start of the 1200 cpsi substrate.

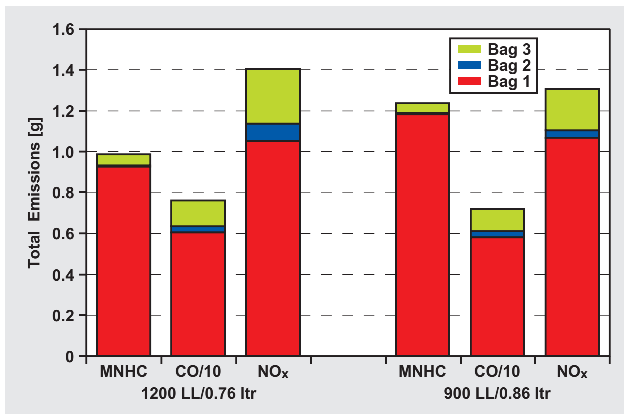

Figure 31: Emission bag data of the 1200 cpsi and 900 cpsi catalyst at same specific loading

Stage 4: 1200 LLL compared to 1200 LL

Besides the 1200 LL catalyst a 1200 cpsi catalyst with the same Rhodium content but a reduced Pd loading level was tested (1200 LLL). The substrate volume was kept constant for both converters.

The catalysts FTP light-off during the FTP cold start is compared in Figure 32. Additionally, the efficiency was recorded during a light-off test on FLEXER at constant mass flow and very low exhaust gas temperature transient (Figure 33). No major difference between the 1200 LL and 1200 LLL converter was realized in both tests. The accumulated tail pipe HC emission during the first phase of the FTP test was lower for the 1200 LL catalyst due to the light-off advantage and the higher efficiency in warmed up condition (Figure 34). The higher efficiency is more visible in Figure 35 showing the HC accumulation during the second phase of the FTP cycle.

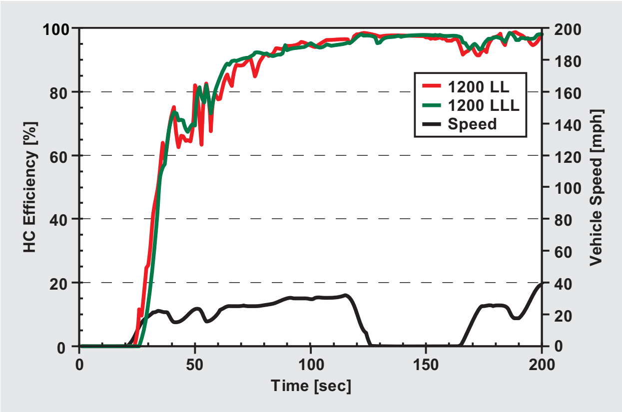

Figure 32: HC-Efficiency during FTP Cold Start for the 1200 LL and the 1200 LLL converter

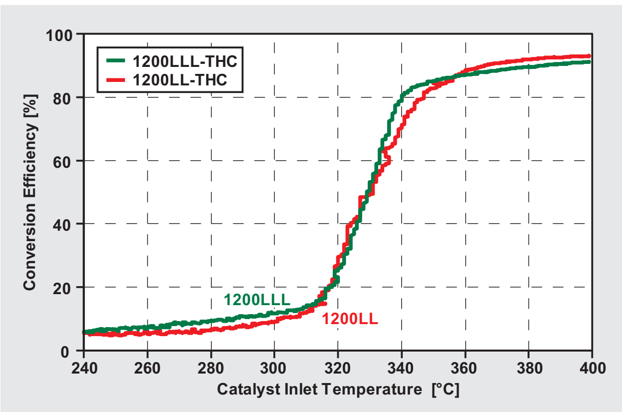

Figure 33: HC- light-off of the 1200 LL and 1200 LLL catalyst after aging (mass flow=20 scfm, AFR=14.67, temperature transient=20 K/min)

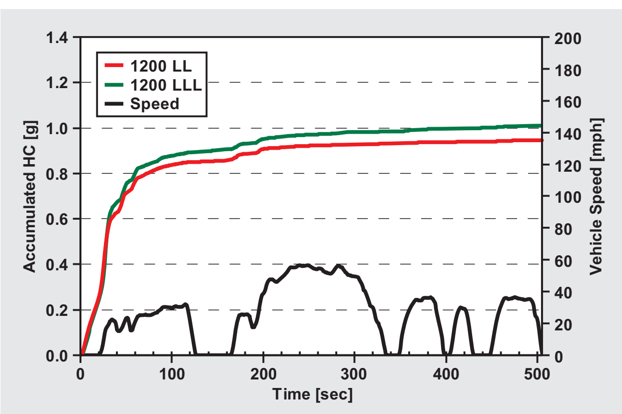

Figure 34: Accumulated HC after the 1200 LLL and 1200 LL catalyst during 1st Phase of the FTP test cycle

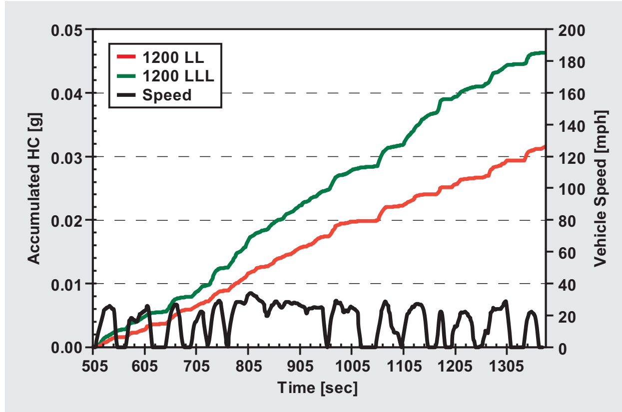

Figure 35: Accumulated HC after the 1200 LLL and 1200 LL catalyst during 2nd Phase of the FTP test cycle

The accumulated CO and NO_X emissions are shown in Figure 36 and Figure 37. The NO_X tail pipe emissions are comparable for both converters. The CO accumulation between 40 and 80 seconds are higher for the 1200 LL converter but very similar after 200 seconds. The total FTP data are compared in Figure 38. The bag one shows lower emissions for the 1200 LL. The CO and NO_X emissions were lower for the 1200 LLL catalyst.

This result does not correlate with the results obtained at the AFR sweep test, which are shown in Figure 39. The HC, CO and NO_X efficiency of the 1200 LLL catalyst was always lower compared to the 1200 LL catalyst.

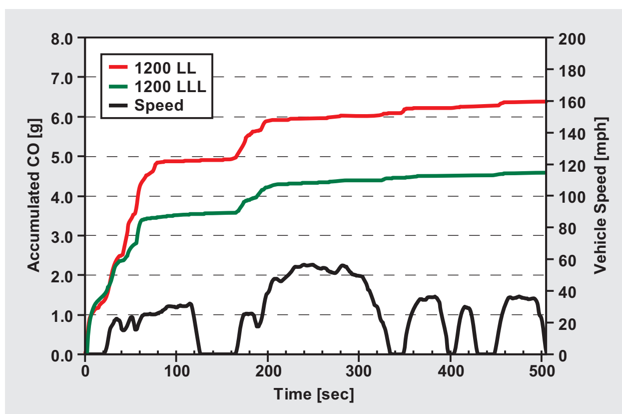

Figure 36: Accumulated CO after the 1200 LLL and 1200 LL catalyst during 1st Phase of the FTP test cycle

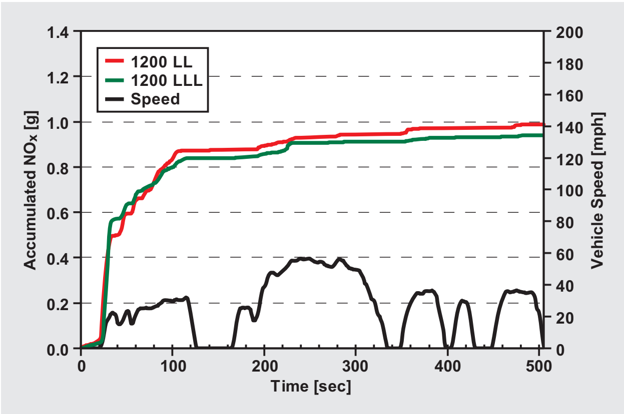

Figure 37: Accumulated NO_X after the 1200 LLL and 1200 LL catalyst during 1st Phase of the FTP test cycle

Overall Summary of FTP Data

The conversion rate during the FTP cold start is compared in Figure 40. All substrates had similar thermal mass per unit volume (compare Table 1). Therefore, a larger active surface is achieved by the advantage of the faster heat up of the 900 cpsi and 1200 cpsi substrate compared to the 500 cpsi substrate. Consequently, a higher efficiency during the first acceleration and between 40 and 80 seconds of the FTP driving cycle was measured and the HC accumulation lower (compare Figure 41).

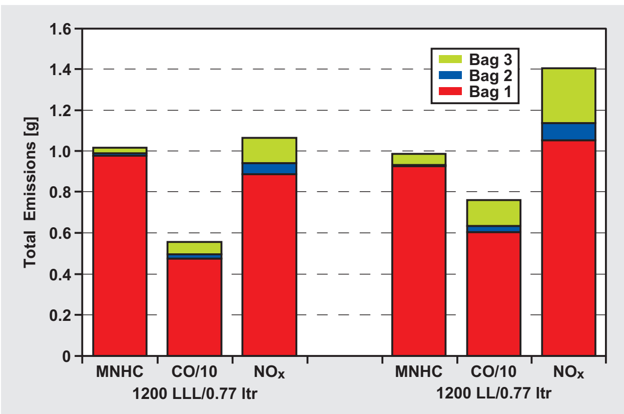

Figure 38: Emission bag data of the 1200 LLL and 1200 LL

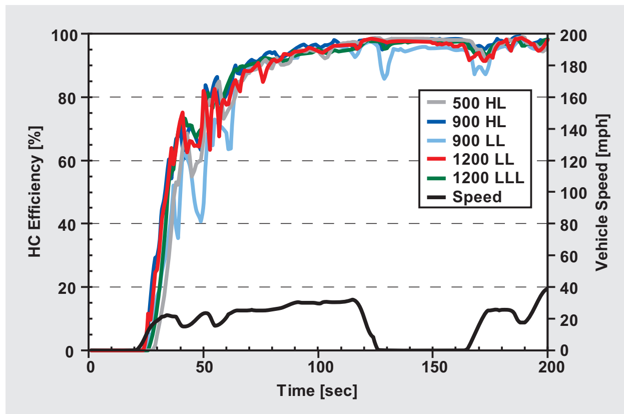

Figure 40: HC light-off of the tested catalyst during FTP Cold Start

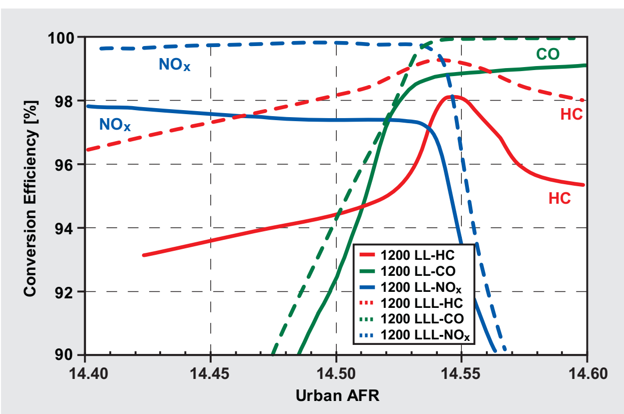

Figure 39: Air/Fuel Sweep – 1200 LLL aged compared to 1200 LL aged (exhaust gas temperature 650 °C, mass flow 49 scfm, AFR perturbation 1Hz, ±1 AFR)

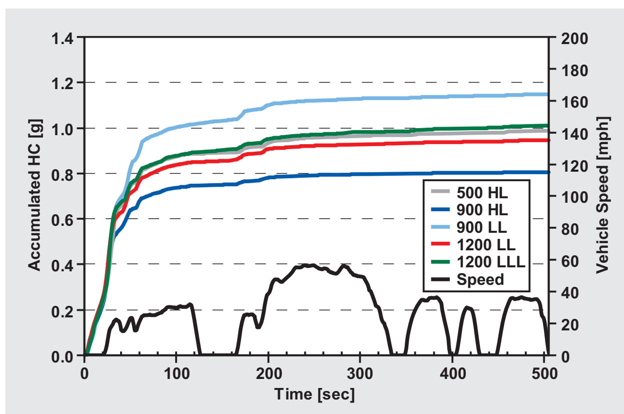

Figure 41: Accumulated THC emissions during the first phase of the FTP cycle

The efficiency is also very much influenced by the Palladium loading. The best light-off performance was achieved with the 900 HL substrate. The THC accumulation of the 900 HL was about 20 % lower and 15 % higher for the 900 LL catalyst compared to the 500 HL catalyst. The 1200 LL catalyst shows a light-off advantage compared to the 900 LL catalyst. The 1200 LLL had the same total thermal mass than the 1200 LL but the lowest Pd loading level. Hence, the light-off is delayed and the efficiency slightly decreased and the accumulation of the THC higher.

The FTP bag data are presented in Figure 42, 43 and 44. The total NMHC and the CO emissions are mainly influenced by the first bag and lower emissions achieved with higher cell density and higher loading.

The NO_X bag data are presented Figure 44. The bag data show no clear trend. The variations of the NO_X performance is influenced by the catalyst bed temperature during the phase where the engine goes in closed loop operation, the values of which are shown

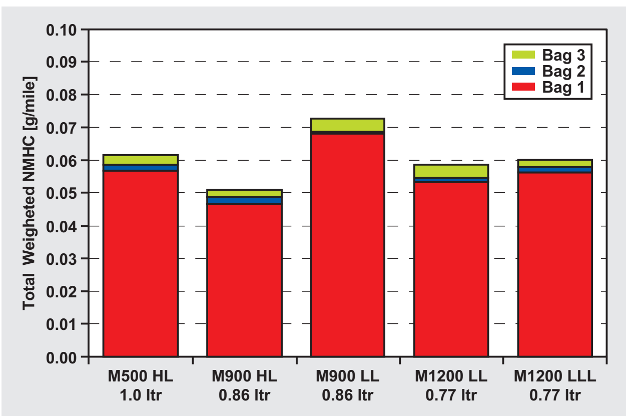

Figure 42: Total weighted NMHC FTP results

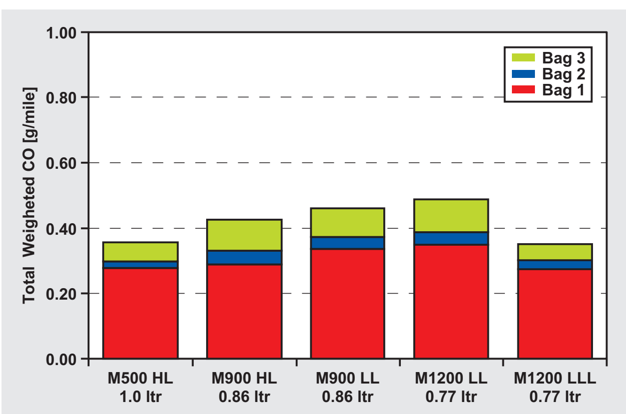

Figure 43: Total weighted CO FTP results

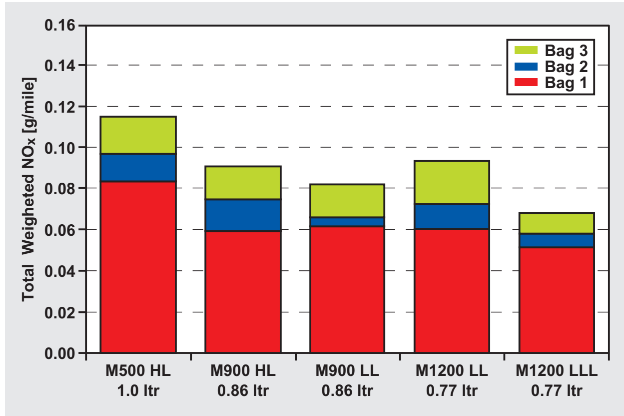

Figure 44: Total weighted NO_X FTP results

in Figure 9 and Figure 10. The NO_X efficiencies for all catalyst were after aging was still between 99.1 % and 99.6 %. Additional emission reductions may be realized by tuning AFR for each catalyst. From the catalyst perspective, the performance of the 1200 LLL catalyst should be worse compared to the 1200 LL. On the other hand the lower Palladium level of the 1200 LLL catalyst allows more CO to be available for the NO_X reducing over the Rhodium. Further testing is required to clarify these statements.

US06 Test Results

The combined NMHC+NO_X bag data are presented in Figure 45. Similar tail pipe emissions were achieved for the 900 cpsi substrates compared to the 500 cpsi substrate. The NO_X emissions of the 500 cpsi and 900 cpsi catalysts are 10 % lower compared to the 1200 cpsi systems. The 1200 LL and 1200 LLL show similar performance.

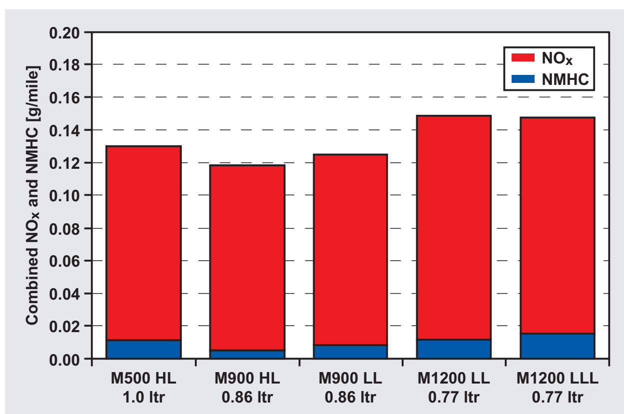

Figure 45: Combined NMHC+NO_X emissions for the US06 test

CONCLUSION

The following overall conclusions can be drawn out of the test program:

- The faster thermal response of the tested 900 HL catalyst showed an emission reduction of 20 % in bag 1 compared to the 500 HL catalyst
- Using high cell density technology increased the light-off performance
- The 1200 cpsi substrate (1200 LL) lights off faster than the 900 cpsi catalyst (900 LL)
- Similar HC and CO warmed-up performance was achieved for the high cell density catalyst compared to the 500 cpsi catalyst
- Similar NO_X efficiency was achieved for 900 LL and 1200 LL catalyst
- No significant differences between the systems in the US06 test were observed
- The smaller hydraulic diameter and better mass transfer of the higher cell density substrates increase the reaction probability and need less precious metals to achieve similar efficiencies
- The light-off advantage of higher cell density catalyst can be used to accomplish lower emission targets or to reduce precious metal loadings compared to standard cell density substrates
- The results of the light-off bench test and the lambda sweep test correlate well with FTP emission performance

The engine AFR was biased to accomplish higher catalyst efficiency during the FTP test cycle for the aged converter. The engine management was not changed during FTP cold start. Therefore, lower tail pipe emissions could be achieved with high cell density through faster heat up and faster light-off. Additional improvements may be realized through individually AFR optimization for each catalyst. Particularly, the NO_X performance could still use improvement for this application between 40 and 100 seconds of the first FTP phase. The reduction of volume and precious metal was fairly small when cell density was increased and therefore no significant differences between the catalysts observed. Usually, higher flow conditions in the US06 cycle show negative impact of thrifting the volume and PGM.

The overall advantage of the high cell density substrates could help to reduce catalyst volume and therefore improve packaging, reduce precious metal cost by achieving equivalent emissions through faster light-off and higher specific efficiency.

REFERENCES

[1] Katherine W. Hughes, Wade Witte, “Ultra Thin Wall Substrates in FTP and US06 Tests”, SAE-Paper 2002-01-0356

[2] Rolf Brueck, Klaus Mueller-Haas, Juergen Breuer, Cynthia Webb, “Advanced Performance of Metallic Converter Systems Demonstrated on a Production V8 Engine”, SAE-Paper 2002-01-0347

[3] J. Schmidt, J. Franz, N. Merdes, Mike Brady, W. Mueller, D. Lindnere, T. Bog, D. Clark, F. Abe, M. Makino, A. Kunz, C.D. Vogt, T. Buckel, W. Stoepler, R. Henninger, E. Ermer, “Utilization of Advanced Three-Way Catalyst Formulations on Ceramic Ultra Thin Wall Substrates for Future Legislation”, SAE-Paper 2002-01-0349

[4] Per Marsh, Dr. Filip Acke, Roman Konieczny, Rolf Brueck, Peter Hirth, “Application Guideline to Define a Catalyst Layout for Maximum Catalytic Efficiency”, SAE-Paper 2001-01-0929

[5] R. Brueck, J. Diringer, U. Martin, W. Maus, “Flow Improved Efficiency by New Cell Structures in Metallic Substrates”, SAE-Paper 950788

[6] Cynthia C. Webb, “ERIC – A System to Modify Vehicle Emissions through Computer Controlled Signal Interception”, SAE-Paper 1999-01-0773

DEFINITIONS, ACRONYMS, ABBREVIATIONS

AFR: Air to Fuel Ratio

CO: Carbon Monoxide

FLEXER: **FL**exible **EX**haust **E**valuation **R**ig

FTP: FEDERAL TEST PROCEDURE

HL: High Load

LL: Low Load

LLL: Low Low Load

NMHC: Non Methan Hydrocarbons

NOx: Oxides of Nitrogen

THC: Total Hydrocarbons

TS: Transversal Structure